# High resolution neutron total cross section measurement of $^{89}$Y†

H. S. Camarda
*Lawrence Livermore Laboratory, University of California, Livermore, California 94550*
(Received 14 March 1977)

Results of a high resolution neutron time-of-flight experiment for neutron energies $27 \leq E \leq 240$ keV on the target nucleus $^{89}$Y ($J^\pi = 1/2^-$) are presented. The measurement employed a 5 nsec beam burst and a 250 m flight path. A multilevel shape analysis of the data was carried out. The parities of almost all observed resonances were easily determined, and for $s$ wave levels the $J$ values of most resonances were obtained. It was found that the $\Sigma\Gamma_n^0$ vs $E$ plot of the $l = 0$, $J = 1$ levels exhibited a significant change in slope over the 240 keV interval, which was interpreted as evidence for a $1^-$ doorway state. The analysis yielded an escape width $\Gamma^\downarrow = 0.8$ keV and a spreading width $\Gamma^\downarrow = 100$ keV, with the doorway state located at a neutron energy of 70 keV. No effect attributable to nonstatistical behavior was observed in the $p$ wave channel. Since most $s$ and $p$ wave levels were observed a relatively clean test could be made of the expected ratio of $s$ to $p$ wave level spacings. After estimating the number of missed levels (inferred through the use of the Porter-Thomas distribution), the experimental ratio of $s$ to $p$ wave spacings was found to be 2.74. This is in disagreement with the theoretical level density prediction of 2.06. The average $s,p$ strength functions and level spacings are $S_0 = 0.28 \pm 0.05 \times 10^{-4}$, $S_1 = 2.64 \pm 0.03 \times 10^{-4}$, $\langle D \rangle_{l=0} = 4.0$ keV, $\langle D \rangle_{l=1} = 1.46$ keV.

[NUCLEAR REACTIONS Neutron total cross section measurement of $^{89}$Y, $27 < E < 240$ keV. Multilevel analysis, determined $E$, $J^\pi$, $\Gamma_n$ of resonances. Deduced $s$ and $p$ wave strength functions, doorway state parameters $E_d$, $\Gamma^\downarrow$, $\Gamma^\downarrow$.]

## INTRODUCTION

Reported here are the results of a high resolution neutron total cross section measurement on the target nucleus $^{89}$Y ($J^\pi = \frac{1}{2}^-$), which was carried out for incident neutron energies $27 \leq E \leq 240$ keV. Yttrium has a closed neutron shell ($N = 50$) and lies near the mass 90 $3P$ maximum of the $p$ wave strength function. In the mass 90 region the $s$ wave strength function exhibits a minimum and it is reasonable to assume that the $d$ wave strength function will be small also. Consequently, only $l = 0$ and $l = 1$ interactions are expected to be important. Previous measurements[1] on $^{89}$Y ($E \leq 30$ keV) implied that the resonance strengths and spacings were such that the best current experimental resolution was capable of resolving a statistically significant number of levels over a several hundred keV energy interval. With good resolution the $s$ and $p$ wave resonances can be identified and the energy dependence of the corresponding strength functions examined. A 200 keV interval is still small enough for any energy dependence of the strength functions, as predicted by the optical model,[2] to be insignificant but large enough for any intermediate energy dependence, e.g., the influence of isolated doorway states,[3] to be observed. Since yttrium has a closed neutron shell and only one proton outside a closed subshell is represents a more favorable case for exhibiting nonstatistical behavior. Furthermore, in addition to determining values of the $s$ and $p$ wave strength functions, the detection and identification of most of the $s$ and $p$ levels provides a clean test of the expected ratio of $s$ to $p$ wave level densities.

## EXPERIMENT

The measurement was carried out with the Lawrence Livermore Laboratory 100 MeV electron linear accelerator (located underground) and employed the time-of-flight (TOF) technique. The electron beam was brought above ground where it struck a water cooled tantalum target. This neutron producing target is viewed by three evacuated flight paths which are 15, 66, and 250 m long. For this measurement the 250 m flight path was used. The accelerator was operated at 720 pps employing a 5 nsec beam width at an average electron current of 25 $\mu$A. The neutron detector, located in a small building at the end of the 250 m flight path, consisted of three 1 cm thick, 12.7 cm diam $^6$Li glass scintillators each coupled to an RCA 4522 phototube. The three detectors were wrapped in a thin aluminum shroud and suspended in the beam line by wires attached to the ceiling of the house. Thus the amount of nonessential mass in the beam was kept to a minimum.

The detector signals were processed by a fast-slow system (the arrival time of the signals was determined by a constant fraction timing discriminator) and fed into a time digitizer interfaced to

an on-line computer.[4] For neutron energies below and above 52 keV, 4 and 2 nsec channel widths were employed, respectively. For the neutron energies covered in this experiment (27–240 keV) this amounted to about 30 000 channels of TOF data. The 5 nsec electron burst width and 250 m flight path gave a nominal resolution of 0.02 nsec/m which is typical of the best resolution attainable with present neutron TOF facilities.

The yttrium samples were 99.9% pure, cylindrical in shape (8.40 cm diam), and had $1/n$ values of 6.00, 11.9, and 25.5 b/atom. The samples were placed 5 m from the neutron producing target where the defining collimators were 7.5 cm in diameter. Estimates of the beam dependent background were made by using Fe filters. These backgrounds were typically 7% and 4% in the 28 and 80 keV energy regions, respectively. Normalization between open and sample runs was determined by fast cycling. In order to eliminate overlap neutrons a $^{10}B$ filter (0.95 g/cm$^2$) was in the beam during all the runs.

After examination of the yttrium TOF data it was apparent that the resolution, although quite good, was not as good as expected. The flat Li glass scintillator had been coupled to the curved surface of the photomultiplier with a plastic adapter. It was therefore concluded that some neutrons which originally passed through the Li glass undetected, underwent moderation in the plastic adapter, reentered the Li glass, and were detected at a later time. To test this conclusion a transmission measurement (5 nsec beam burst, 15 m flight path, 2 nsec channels) on Fe was performed using the Li glass detector, with plastic and quartz adapters (but otherwise having equal neutron pulse heights), under identical conditions. Although a quantitative analysis was not carried out, the shapes of the Fe resonances clearly demonstrated that the Li glass with the quartz adapter gave superior resolution.

## ANALYSIS

The first step in the analysis is to process the raw data into a transmission vs energy format. This was done after making dead time corrections, subtracting backgrounds, and normalizing open to sample in runs.

The nature of the data (see Fig. 1) is such that many levels overlap strongly and the $s$ wave levels evidence rather dramatic interference effects. Area analysis of overlapping levels is not useful and $s$ wave levels with strong interference effects result in a small net experimental area which can cause large uncertainties in the resonance widths. Consequently a multilevel shape analysis was pursued. An $R$-matrix analysis which correctly treats coherent interference between resonances was not carried out because, for $Y$, few levels with the same spin and parity are expected to have significant overlap. Instead, a multilevel analysis consisting of a sum of $l=0$ and $l=1$ Breit-Wigner equations, which included the effects of Doppler broadening and instrumental resolution, was pursued. Specifically,

$$\sigma_t = \sigma_0 + \sigma_1 , \tag{1a}$$

$$\sigma_0 = 4\pi\lambda^2 \sum_J [g_J(\Gamma_n^s)_J/\Gamma_J^s] \cos 2\gamma_0 \times \{\psi(B_J, X_J) + \tan 2\gamma_0 \chi(B_J, X_J)\} + 4\pi\lambda^2 \sin^2\gamma_0 , \tag{1b}$$

$$\sigma_1 = 4\pi\lambda^2 \sum_J [g_J(\Gamma_n^p)_J/\Gamma_J^p] \cos 2\gamma_1 \psi(B_J, X_J) + 4\pi\lambda^2 (3\sin^2\gamma_1) , \tag{1c}$$

$$\Gamma_n^s = (E/1\text{ eV})^{1/2}\Gamma_n^0 , \tag{1d}$$

$$\Gamma_n^p = (E/1\text{ eV})^{1/2}\{y^2/(1+y^2)\}\Gamma_n^1 , \quad y = kR , \tag{1e}$$

$$\Gamma = \Gamma_n + \Gamma_\gamma , \tag{1f}$$

$$X_J = 2(E - E_J)/\Gamma_J , \tag{1g}$$

$$B = 2\Delta/\Gamma , \quad \Delta = (E/10A)^{1/2} , \tag{1h}$$

$$\gamma_0 = kR' , \quad R' = R(1 - R_0^\infty) , \tag{1i}$$

$$\gamma_1 = \phi_1 + \theta_1 , \tag{1j}$$

$$\phi_1 = \tan^{-1}[-j_1(y)/\eta_1(y)] , \tag{1k}$$

$$\theta_1 = \tan^{-1}[-R_1^\infty P_1/(1 - R_1^\infty S_1)] , \tag{1l}$$

$$P_1 = y^3/(1+y^2), \quad S_1 = y^2/(1+y^2) . \tag{1m}$$

The form of the cross section above and the definitions of the different parameters result from an $R$-matrix[5] derivation of the Breit-Wigner equation. $\sigma_0$ and $\sigma_1$ represent the $s$ and $p$ wave contributions to the total cross section. $\Gamma_n$, $\Gamma_\gamma$, $E_J$, and $g_J$ are the neutron width, capture width (assumed to be 0.3 eV for all levels), resonance energy, and spin factor associated with each resonance. For the $l=1$ case a self-interference term, similar to the $l=0$ term $[\sin 2\gamma_0\chi(B_J, X_J)]$ was not included because it is negligible for neutron energies $\lesssim$240 keV. With a nuclear radius $R$ equal to 6.23 fm, $R_0^\infty$ and $R_1^\infty$ were found to be $-0.23$ and 0.00, respectively. The values are consistent with previous measurements.[6] $R_0^\infty$ was allowed to vary by $\pm 10\%$ in different energy regions. $\psi(B, X)$ and $\chi(B, X)$ are the Doppler-broadening integrals which replace $1/(1+X^2)$ and $X/(1+X^2)$ in the normal Briet-Wigner equation. Finally, the experimentally observed trasmission was calculated by convoluting the transmission $T = \exp(-n\sigma_t)$ with a re-

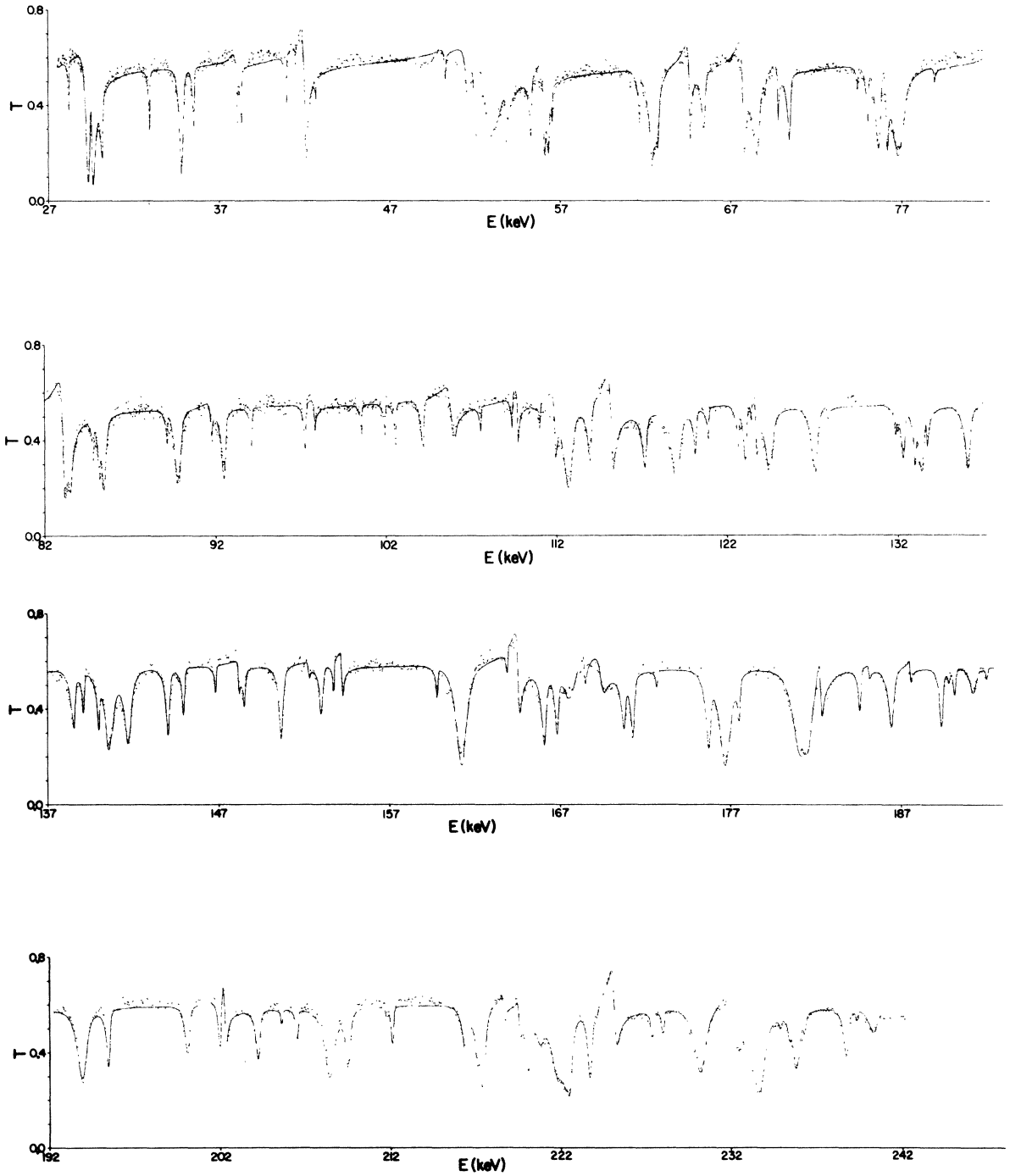


FIG. 1. (a), (b) Transmission vs. neutron energy for the $1/n = 11.9$ b/atom sample of $^{89}$Y. The smooth curve was generated from a multilevel analysis as described in the text.

solution function. The shape of the resolution function was determined by examining how the narrow levels were smeared at different energies. It was found that a Gaussian plus a $\chi^2$ distribution with a few degrees of freedom gave a satisfactory representation of the resolution function. The energy dependence was reproduced by different weightings of the Gaussian vs $\chi^2$ part of the expression.

The main purpose of the analysis was to obtain $\Gamma_n$, $E$, parity, and where possible the spins of the levels. The thick sample data ($1/n = 6.00$) were used mainly to detect weak resonances and to help

TABLE I. $l=0$ resonance parameters of $^{89}$Y. Level with the symbol † are of undetermined parity.

| $E$ (keV) | $g\Gamma_n$ (eV) | $J$ | $E$ (keV) | $g\Gamma_n$ (eV) | $J$ |
|---|---|---|---|---|---|
| 29.620 ± 0.007 | 56.3 ± 8 | 1 | 115.28 ± 0.02 | 109 ± 15 | 1 |
| 38.075 ± 0.010 | 9.0 ± 2 | 1 | 123.73 ± 0.02 | 49 ± 6 | 1 |
| †41.527 ± 0.020 | 1.8 ± 0.5 | | 127.90 ± 0.03 | 7.5 ± 3 | |
| 42.135 ± 0.010 | 45.5 ± 5 | 1 | 133.68 ± 0.03 | 24 ± 3.6 | 1 |
| †50.295 ± 0.015 | 3.8 ± 2 | | 148.15 ± 0.02 | 17 ± 2.5 | 1 |
| 52.900 ± 0.020 | 200 ± 30 | 0 | †152.28 ± 0.02 | 10 ± 3.5 | |
| 53.890 ± 0.007 | 18.8 ± 3 | 1 | 154.22 ± 0.03 | 30 ± 5 | 1 |
| 56.120 ± 0.010 | 27 ± 6 | 1 | 164.63 ± 0.03 | 105 ± 15 | 1 |
| 64.675 ± 0.010 | 35 ± 4 | 1 | 168.48 ± 0.03 | 20 ± 4 | |
| 67.830 ± 0.012 | 56 ± 9 | 1 | 169.48 ± 0.04 | 100 ± 15 | 0 |
| 69.825 ± 0.010 | 16.5 ± 4 | 1 | 182.31 ± 0.04 | 82 ± 15 | 1 |
| 76.210 ± 0.010 | 45 ± 9 | 1 | 185.11 ± 0.04 | 12 ± 4 | |
| 79.000 ± 0.015 | 3.7 ± 1.3 | | 187.52 ± 0.04 | 15 ± 3 | |
| 83.150 ± 0.015 | 93 ± 20 | 1 | 202.26 ± 0.06 | 71 ± 10 | 1 |
| 91.750 ± 0.015 | 13.5 ± 3 | | 218.57 ± 0.08 | 23 ± 4.5 | 1 |
| 97.820 ± 0.015 | 13.8 ± 3 | | 219.50 ± 0.08 | 26 ± 8 | 1 |
| 105.92 ± 0.03 | 70.0 ± 10 | 0 | 225.13 ± 0.05 | 150 ± 22 | 1 |
| 109.72 ± 0.02 | 26 ± 5 | | 232.21 ± 0.05 | 135 ± 35 | 1 |
| 111.92 ± 0.02 | 41 ± 7 | 1 | | | |

identify the parity of these levels. For the shape analysis of the data the $1/n = 11.9$, 25.5 b/atom samples were emphasized. They have the advantage of being less sensitive to uncertainties in the background and resolution function.

In Figs. 1(a) and 1(b) is plotted the experimental transmission vs neutron energy (data points), along with the multilevel fit (smooth curve) for the sample $1/n = 11.9$. Equivalent fits were obtained for the $1/n = 25.5$ sample. These plots indicate the nature of the observed structure and the quality of the fits to the data. Except for the smallest levels it was easy to distinguish $s$ from $p$ levels. The spin ($J = 0, 1$) for most $l = 0$ resonances was apparent from the fitting procedure. Similarly, $p$ levels with $J = 0$ as opposed to $J = 1, 2$ could be identified but it was not possible to cleanly separate $J = 1$ and $J = 2$ $p$ wave resonances. Tables I and II list the $l = 0$ and $l = 1$ resonance parameters, respectively. Levels for which a parity assignment could not be made are denoted by the symbol †. The widths of several $p$ wave transmission dips were too broad to be caused by a single level. In these cases it was necessary to assume that more than one level was contributing. These are identified by an * in Table II; a combined $g\Gamma_n$ value is given because the combination of levels used is not necessarily unique. $J = 0$ $p$ wave levels are denoted by the symbol a. The uncertainties of the parameters were found by noting the acceptable range of $g\Gamma_n$ values for each level in trying to achieve a satisfactory fit. The uncertainties are typically 15% and are appropriately larger where less satisfactory fits were obtained.

There is some overlap at the low energy end of this measurement with the work of Morgenstern *et al.*[1] The $g\Gamma_n$ values of the resonances at 28.196, 29.620, and 29.355 keV agree to within the quoted errors. For the level at 30.130 keV the $g\Gamma_n$ value of 22 ± 3.5 eV found here is lower than their value of 32 ± 4. The parity assignments are in full agreement and the spin $J = 1$ quoted for the $l = 0$ level at 29.620 keV was also found here. In Figs. 2–4, the data below 27 keV is taken from Ref. 1. Of the nine weak $s$ levels with undetermined spin (see Table I), three were arbitrarily assigned to $J = 0$ and six to $J = 1$ in order to include all the data in the $\sum \Gamma_n^0$ vs $E$ plots.

## RESULTS

The slope of a $\sum \Gamma_n^0$ vs $E$ plot, which should be constant in the absence of intermediate structure, determines the value of the strength function. Figure 2(a) shows the behavior of $\sum \Gamma_n^0$ vs $E$ for the $J = 0$ $s$ wave levels. The slope of the straight line yields a strength function of $S_0 = 0.26 \times 10^{-4}$. The statistical uncertainty is estimated to be $\pm 0.15 \times 10^{-4}$. An interesting feature of the data is that about one-half the strength is concentrated in the level at 52.900 keV which has a reduced neutron width of 3.5 eV. If the $J = 0$ level spacing is estimated to be 16 keV, (see below) a width of 3.5 eV would be $8\frac{1}{2}$ times the expected average strength

TABLE II. $l=1$ resonance parameters of $^{89}$Y. Levels with the symbol † are of undetermined parity while those with the symbol * are multiple resonances. $J=0$ $p$ wave levels are denoted by the symbol a.

| $E$ (keV) | $g\Gamma_n$ (eV) | $E$ (keV) | $g\Gamma_n$ (eV) |
|---|---|---|---|
| 28.196 ± 0.004 | 6.9 ± 1.3 | 138.54 ± 0.02 | 83 ± 9 |
| 29.355 ± 0.004 | 71 ± 10 | 139.11 ± 0.02 | 38 ± 6 |
| 30.130 ± 0.004 | 22 ± 3.5 | 140.00 ± 0.02 | 50 ± 7 |
| 32.940 ± 0.005 | 11.3 ± 1.5 | 140.67 ± 0.03 | 263 ± 30 |
| 34.830 ± 0.006 | 54 ± 8 | 141.76 ± 0.03 | 191 ± 25 |
| 35.545 ± 0.006 | 15 ± 2.5 | 144.06 ± 0.03 | 109 ± 11 |
| 38.347 ± 0.006 | 15 ± 3 | 144.95 ± 0.03 | 53 ± 6 |
| 41.000 ± 0.006 | 10 ± 2.5 | 146.82 ± 0.03 | 21 ± 4 |
| 42.725 ± 0.008 | 3 ± 1 | 148.50 ± 0.03 | 37 ± 7 |
| 51.725 ± 0.010 | 50 ± 8 | 150.70 ± 0.03 | 130 ± 13 |
| 52.175 ± 0.010 | 53 ± 8 | 153.04 ± 0.03 | 67 ± 7 |
| 55.350 ± 0.007 | 31 ± 4.5 | 153.74 ± 0.03 | 26 ± 4 |
| 56.380 ± 0.010 | 42.5 ± 8 | 159.83 ± 0.03 | 25 ± 7 |
| 56.600 ± 0.010 | 12.5 ± 3 | 161.34 ± 0.03 | 500 ± 85 |
| 61.700 ± 0.010 | 22 ± 4 | 163.95 ± 0.03 | 19 ± 5 |
| *62.60 ± 0.05 | 176 ± 30 | 166.14 ± 0.03 | 169 ± 16 |
| 65.500 ± 0.010 | 45 ± 7 | 166.89 ± 0.04 | 103 ± 20 |
| *68.600 ± 0.05 | 125 ± 25 | [a]167.65 ± 0.05 | 162 ± 30 |
| 69.065 ± 0.010 | 4.4 ± 1.7 | 170.80 ± 0.04 | 94 ± 18 |
| 70.510 ± 0.012 | 50 ± 7.5 | 171.33 ± 0.04 | 125 ± 17 |
| 74.500 ± 0.015 | 7.5 ± 2 | 172.72 ± 0.04 | 15 ± 4 |
| 75.115 ± 0.015 | 31 ± 7 | 175.79 ± 0.04 | 175 ± 35 |
| 75.765 ± 0.015 | 105 ± 20 | 176.78 ± 0.04 | 550 ± 60 |
| *76.93 ± 0.04 | 188 ± 30 | 177.55 ± 0.04 | 62 ± 10 |
| 83.50 ± 0.02 | 100 ± 20 | *181.14 ± 0.06 | 863 ± 150 |
| 83.53 ± 0.02 | 20 ± 5 | 184.58 ± 0.04 | 56 ± 7 |
| 84.850 ± 0.018 | 20 ± 3.5 | 186.45 ± 0.04 | 150 ± 20 |
| 85.210 ± 0.018 | 28 ± 5 | 189.40 ± 0.04 | 100 ± 12 |
| 85.510 ± 0.018 | 105 ± 18 | †189.83 ± 0.05 | 10 ± 4 |
| 89.150 ± 0.020 | 12.5 ± 3.5 | 190.13 ± 0.04 | 31 ± 4 |
| 89.840 ± 0.020 | 124 ± 18.6 | [a]191.25 ± 0.05 | 75 ± 12 |
| 92.535 ± 0.020 | 79 ± 12 | †192.00 ± 0.04 | 10 ± 3 |
| 94.125 ± 0.020 | 21 ± 4 | 193.93 ± 0.04 | 330 ± 40 |
| 97.270 ± 0.020 | 31 ± 5 | 195.43 ± 0.04 | 100 ± 17 |
| 100.58 ± 0.02 | 15 ± 4 | 200.65 ± 0.04 | 105 ± 17 |
| 101.95 ± 0.02 | 16 ± 4 | 201.96 ± 0.04 | 88 ± 15 |
| 102.58 ± 0.02 | 27.5 ± 6 | 204.20 ± 0.04 | 101 ± 15 |
| 104.17 ± 0.01 | 50 ± 7 | 205.60 ± 0.04 | 15 ± 4 |
| 107.55 ± 0.02 | 12 ± 4 | 206.50 ± 0.04 | 37 ± 6 |
| 109.40 ± 0.03 | 19 ± 6 | 208.44 ± 0.04 | 375 ± 56 |
| 111.00 ± 0.03 | 18 ± 6 | 209.48 ± 0.04 | 135 ± 15 |
| 112.78 ± 0.02 | 218 ± 30 | †211.75 ± 0.04 | 5 ± 2 |
| 113.99 ± 0.02 | 83 ± 12 | 212.07 ± 0.04 | 53 ± 6 |
| 117.20 ± 0.02 | 83 ± 17 | 216.43 ± 0.05 | 161 ± 24 |
| 119.08 ± 0.03 | 210 ± 40 | 217.04 ± 0.06 | 52 ± 15 |
| 120.17 ± 0.02 | 50 ± 7 | 217.37 ± 0.05 | 300 ± 40 |
| 120.93 ± 0.02 | 25 ± 5 | 220.05 ± 0.05 | 172 ± 20 |
| 122.68 ± 0.03 | 31 ± 8 | [a]220.77 ± 0.05 | 100 ± 20 |
| 123.12 ± 0.02 | 88 ± 13 | 221.86 ± 0.05 | 560 ± 80 |
| †123.45 ± 0.03 | 16 ± 5 | 222.20 ± 0.06 | 31 ± 10 |
| 124.57 ± 0.04 | 150 ± 35 | 222.45 ± 0.06 | 288 ± 50 |
| 127.20 ± 0.02 | 150 ± 15 | 223.69 ± 0.05 | 206 ± 20 |
| 131.85 ± 0.04 | 12.5 ± 3.5 | 224.10 ± 0.06 | 12.5 ± 3.5 |
| †131.98 ± 0.04 | 8 ± 3.5 | 227.33 ± 0.05 | 37 ± 6 |
| 132.33 ± 0.03 | 71 ± 11 | 227.95 ± 0.05 | 30 ± 5 |
| 133.00 ± 0.02 | 50 ± 8 | 230.16 ± 0.05 | 450 ± 60 |
| 133.42 ± 0.02 | 172 ± 25 | 232.78 ± 0.06 | 16 ± 7 |
| 136.12 ± 0.02 | 124 ± 13 | 233.12 ± 0.06 | 41 ± 13 |

TABLE II. (*Continued*)

| $E$ (keV) | $g\Gamma_n$ (eV) | $E$ (keV) | $g\Gamma_n$ (eV) |
|---|---|---|---|
| 233.60 ± 0.05 | 600 ± 120 | 236.26 ± 0.05 | 20 ± 6 |
| 234.83 ± 0.05 | 12.5 ± 4 | 238.68 ± 0.05 | 116 ± 15 |
| 235.35 ± 0.06 | 19 ± 5 | 239.32 ± 0.06 | 12 ± 4 |
| 235.78 ± 0.05 | 240 ± 30 | [a]240.30 ± 0.06 | 100 ± 25 |

of 0.4 eV. The Porter-Thomas[7] (PT) distribution predicts that the probability of this occurring is <0.5%.

The plot of $\sum\Gamma_n^0$ vs $E$ for the $J=1$, $l=0$ resonances [Fig. 2(b)] gives clear evidence of an energy variation of the strength function over a 100 keV energy interval. Similar observations have recently been made on other nuclei near or at closed shells.[8,9] It will be assumed here that the energy modulation of the strength function, as depicted in Fig. 2(b), is the result of an isolated $1^-$ doorway state. In the past few years calculations have been performed[10,11] with the aim of examining the possible existence of doorway states in $^{90}$Y which would be observable in an $n+{}^{89}$Y total cross section measurement. In order to facilitate a comparison between theory and experiment it is important to determine the escape width $\Gamma^\uparrow$ and the spreading width $\Gamma^\downarrow$ of the observed structure.

The average behavior (that is, fluctuations due to coupling of doorway states to more complicated configurations smoothed out) of the strength function as a result of an isolated doorway state is[3]

$$(E/1\text{ eV})^{1/2}S^\uparrow = 1/2\pi\frac{\Gamma^\uparrow\Gamma}{(E-E_d)^2+(\frac{1}{2}\Gamma)^2}, \quad \Gamma=\Gamma^\uparrow+\Gamma^\downarrow, \tag{2}$$

where $S^\uparrow$ is the strength function due to an isolated doorway state, $E, E_d$ are the neutron and doorway state energy, and $\Gamma$ the total width. The escape width is given by the expression[3]: $\Gamma^\uparrow = 2\pi\rho(E) \times |\langle\chi^+|V|\psi_d\rangle|^2$ where $|\chi\rangle$, $|\psi_d\rangle$ are the entrance channel and doorway state wave functions, which are coupled by the two body residual interaction $V$. For the target nucleus $^{89}$Y and for the incident neutron energies of this experiment, $\Gamma^\uparrow = \Gamma_n^\uparrow$. For a low energy $l=0$ neutron the product $\rho(E)(\chi^+)^2$ has a $\sqrt{E}$ dependence. Therefore, the escape width is defined in terms of a reduced width $\Gamma_R^\uparrow$, i.e., $\Gamma^\uparrow = \sqrt{E}\Gamma_R^\uparrow$. Let the observed strength function be represented by a resonance term and a constant "background" term $S_0'$. Then, the sum of reduced widths as a function of neutron energy $E$ takes the form:

$$\sum\Gamma_n^0 = S_0'E + \frac{1}{2\pi}\int_0^E \frac{\Gamma_n^\uparrow\Gamma\,dE}{(E-E_d)^2+(\frac{1}{2}\Gamma)^2}$$
$$\Gamma = (E/1\text{ eV})^{1/2}\Gamma_R^\uparrow + \Gamma^\downarrow. \tag{3}$$

Using this expression the parameters $S_0'$, $E_d$, $\Gamma_R^\uparrow$, and $\Gamma^\downarrow$ were varied in order to find a satisfactory fit to the data displayed in Fig. 2(b). The smooth curve of Fig. 2(b) was calculated with the parameters $S_0' = 0.15\times10^{-4}$, $E_d = 70$ keV, $\Gamma_R^\uparrow = 3$ eV ($\Gamma^\uparrow = 0.8$ keV), and $\Gamma^\downarrow = 100$ keV. The corresponding uncertainties are $\pm0.05\times10^{-4}$, ±10 keV, ±1.5 eV, and ±35 keV.

Ramavataram *et al.*[10] performed a calculation examining possible structure in the $^{89}$Y total neutron cross section arising from doorway states ($0^-$, $1^-$, $2^-$) accessible to $s$ and $d$ wave neutrons. The model vector space for these calculations

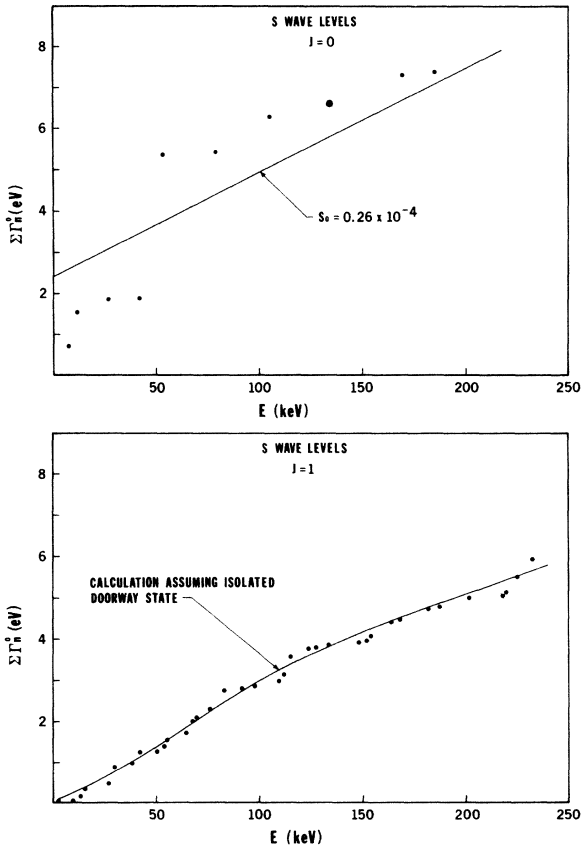


FIG. 2. (a), (b) $\sum\Gamma_n^0$ vs $E$ for the $s$ wave $J=0$ and $J=1$ resonances. The data below 27 keV is from Ref. 1. The smooth curve through the $J=1$ data was calculated assuming the existence of an isolated doorway state (see text).

included 2p and 3p-1h states and possible configuration mixing between them. The 3p-1h states could couple to more complicated 4p-2h states through the residual two body interaction. Although higher incident neutron energies ($E > 900$ keV) were emphasized, these authors noted that the calculations indicated the existence of an isolated (to within 300 keV) $1^-$ doorway state in $^{90}$Y at an excitation energy of 7.05 MeV. This energy agrees sufficiently well with the 6.93 MeV $1^-$ state found here. However, the calculated escape width is about an order of magnitude less than the value $\Gamma^\dagger = 0.8$ keV found here and, in addition, no estimate of the spreading width is given.

The results above suggest the existence of a $1^-$ doorway state at an excitation energy of 6.93 MeV in $^{90}$Y. $^{90}$Y is the parent ($T, T_z = 6, 6$) of highly excited analog states ($T, T_z = 6, 5$) of $^{90}$Zr, and a 6.93 MeV excitation in $^{90}$Y corresponds to a 20.06 MeV excitation in $^{90}$Zr. Structure has been found in the $^{89}$Y$(p, \gamma_0)^{90}$Zr cross section at high excitation energies.[12] However, the closest prominent structure to 20.06 MeV excitation lies at 19.4 MeV. Since the Coulomb energy differences are known to better than 100 keV, this energy difference is too great to associate the $1^-$ state found here with any of those in $^{90}$Zr. The $^{89}$Y$(p, \gamma_0)^{90}$Zr measurements are sensitive to states which can be formed by dipole absorption of a $\gamma$ ray by $^{90}$Zr; as a result, it is probably more appropriate to examine the $^{89}$Y$(p, p)$ cross section. These measurements[12] are suggestive of structure in the $^{89}$Y$(p, p)$ cross section at 20.0 MeV excitation but the energy resolution of the data is not sufficient to reach any definite conclusion.

For the $p$ wave levels the graph of $\sum g\Gamma_n^1$ vs $E$ of Fig. 3 does not exhibit any unusual behavior. A value of $S_1 = 2.64 \times 10^{-4}$ is determined by the straight line drawn through the data and the statistical uncertainty is $\pm 0.03 \times 10^{-4}$. The previous value of $S_1$ determined by Morgenstern *et al.*[1] with data to 30 keV was $S_1 = 4.4 \pm {}^{2.0}_{1.2} \times 10^{-4}$. The value of $S_1$ found here represents a substantial improvement in statistical precision.

It is interesting to compare the experimental and theoretical ratio of $s$ wave to $p$ wave level spacings. First the number of missing levels must be estimated; to this end the PT distribution for the reduced widths is used as a diagnostic tool.

In the $l = 0$ case the average reduced width of the PT distribution is given by $\langle g\Gamma_n^0 \rangle = S_0 \Delta E / N_s$. A representative value of $S_0$ for the $\Delta E = 240$ keV energy interval is $0.28 \times 10^{-4}$. Since $S_0$ and $\Delta E$ are known, the only free parameter is the true number of $s$ levels $N_s$. $N_s$ is varied until a reasonable fit to the data is obtained. The histogram of Fig. 4(a) represents the experimental distribution of reduced widths for the $l = 0$ levels and the solid and dashed curves are the PT fits with $N_s = 60$ and 70. The value of $N_s = 60$ gives a reasonable fit to the data, leading to $\langle D \rangle_{l=0} = 4.0$ keV. (Assuming a $2J + 1$ level density dependence, this implies a 16 and 5.3 keV $J = 0$ and $J + 1$ $s$ wave level spacing, respectively.)

The expected combined spin ($J = 0, 1, 2$) distribution of reduced $p$ wave widths is more complicated than in the $l = 0$ case. Resonances with $J = 0$ and 2 can be formed only through the $p_{1/2}$ and $p_{3/2}$ spin-orbit channels, respectively; an optical model calculation[6] indicates the average reduced width $\langle g\Gamma_n^1 \rangle$ for these levels should differ by a factor of 2. In addition, as previously noted,[13] resonances of a given $J$ which can be formed through both the $p_{1/2}$ and $p_{3/2}$ channels do not obey a single channel PT distribution. The $J = 1$ $p$ wave levels of $^{89}$Y can be formed through both the $p_{1/2}$ and $p_{3/2}$ channels (i.e., $\Gamma_{J=1} = \Gamma_{p_{1/2}} + \Gamma_{p_{3/2}}$) and, as mentioned above, should have different average widths. For equal widths a $\chi^2$ distribution of two degrees of freedom would apply. For the assumed unequal widths here Monte Carlo methods were used to generate the reduced width distribution of the $J = 1$ levels. The distribution of $p$ wave reduced widths for combined spin took the form:

$$P(x)dx = \tfrac{1}{9} N_p [P_0(x) + 3P_1(x) + 5P_2(x)]dx, \quad x = (g\Gamma_n^1)^{1/2}, \tag{3a}$$

$$\langle g\Gamma_n^1 \rangle_{J=2} = \frac{27\Delta E}{4N_p} S_1 \frac{R}{(2R+1)}, \quad \langle g\Gamma_n^1 \rangle_{J=0} = \frac{1}{R} \langle g\Gamma_n^1 \rangle_{J=2} \tag{3b}$$

$$\langle g\Gamma_n^1 \rangle_{J=1} = \langle g\Gamma_n^1 \rangle_{J=0} + \langle g\Gamma_n^1 \rangle_{J=2} \tag{3c}$$

This expression assumes the validity of the $2J + 1$ level density dependence. $S_1$ is the measured strength function of $2.64 \times 10^{-4}$ found over the energy interval $\Delta E = 240$ keV and $R$ is the ratio of the $p_{3/2}$ to $p_{1/2}$ strength functions ($R = 2$ was used). $P_0$,

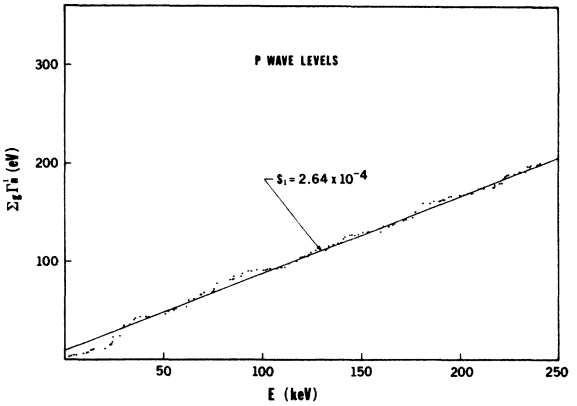


FIG. 3. $\sum g\Gamma_n^1$ vs $E$ for the $p$ wave levels (all spins). The data below 27 keV are from Ref. 1.

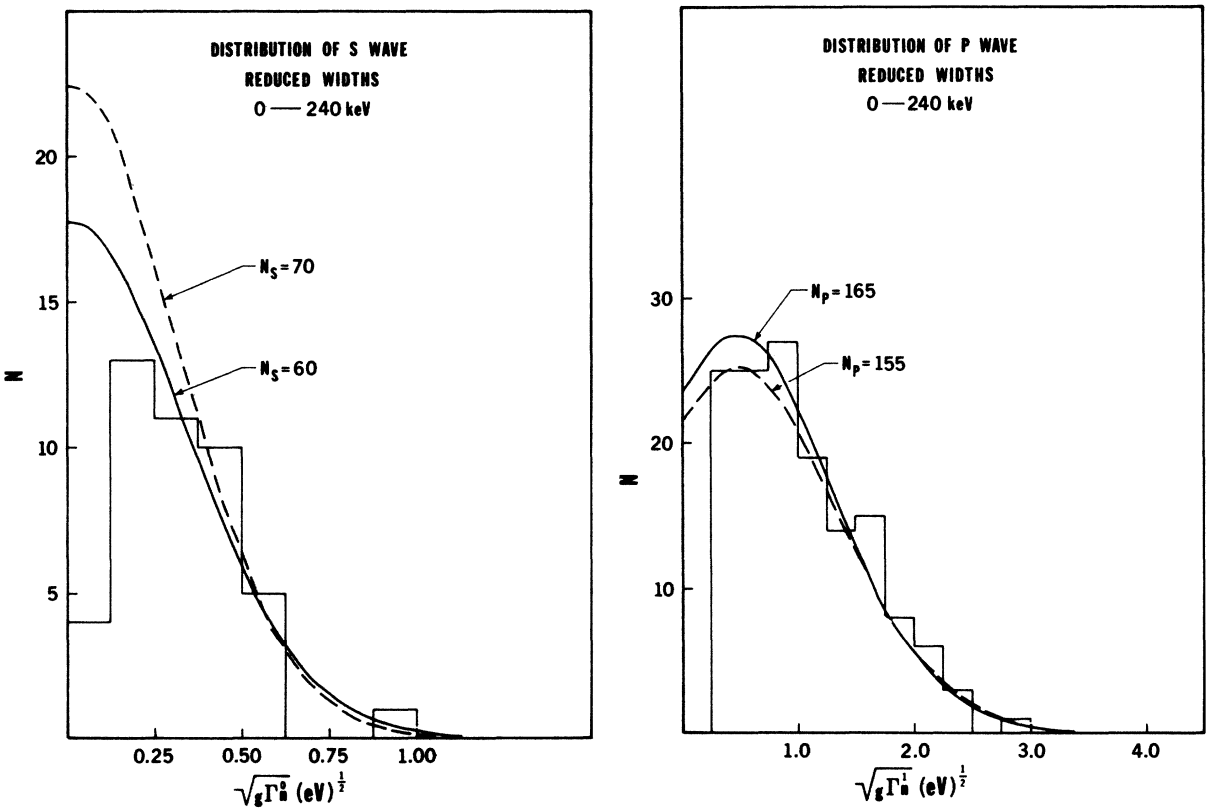


FIG. 4. (a), (b) Histograms represent the experimental distribution of reduced widths while the smooth curves give the expected distribution for different values of the true number of levels.

$P_1$, and $P_2$ are the probability distributions for the $J = 0$, 1, and 2 reduced widths. The only free parameter is $N_p$, the true number of $p$ levels, and it was varied until a satisfactory fit was obtained. The histogram of Fig. 4(b) represents the experimental reduced widths and the solid and dashed curves are the expected distributions with $N_p = 165$ and 155, respectively. One notes that the theoretical distribution does not peak as $x \to 0$ but instead "turns over." This is the effect of the two channel distribution of the $J = 1$ levels. A satisfactory fit is obtained with $N_p = 165$ and gives a corrected $p$ wave level spacing of $\langle D \rangle_{l=1} = 1.46$ keV. Therefore the experimental ratio of $s$ wave to $p$ wave level spacings is 2.74.

Bethe's expression for the level density as given by Gilbert and Cameron,[14] has the form

$$\rho(J, U, A) = \frac{C(U, A)}{\sigma^3}(2J+1)\exp[-(J+\tfrac{1}{2})^2/2\sigma^2]. \quad (4)$$

$\rho$ is the number of levels of a given $J^\pi$ per unit energy interval for a nucleus with $A$ nucleons at excitation energy $U$. $\sigma$ is the spin cutoff factor. The functional form of the expression above still results (for $J$ not too large) when more sophisticated models are employed.[15] These models introduce in a natural way, odd-even effects in the nuclear excitation energy and the influence of shell structure on $C(U, A)$ and $\sigma$. A comparison of the number of $s$ and $p$ levels at the same excitation energy in a given nucleus tests the factor $(2J+1)\exp[-(J+\frac{1}{2})^2/2\sigma^2]$ and the assumption of parity independence of the level density expression. For $\sigma = 3.8$, a typical value for the mass 90 region,[14,15] the expected ratio of $s$ to $p$ wave level spacing is 2.06. If $\sigma = \infty$, the expected ratio is 2.25. These values differ significantly from the experimental result of 2.74. By increasing the number of $s$ levels to 70 and decreasing the $p$ levels to 155, the experimental ratio becomes 2.21. As can be seen from Fig. 4(a), $N_s = 70$ is highly improbable and, furthermore, still yields a result in disagreement with the finite $\sigma$ prediction. Therefore it is reasonable to conclude that the assumption of parity independence of the level density or the $J$ dependence expression may not be applicable to $^{90}$Y at excitations near the neutron binding energy.

I would like to thank J. C. Browne for the use of his data taking program and for useful discussions. My thanks to A. K. Kerman for an informative discussion.

†Work performed under the auspices of the U. S. Energy Research and Development: W-7405-Eng-48.

[1]J. Morgenstern, R. N. Alves, J. Julien, and C. Samour, Nucl. Phys. A123, 561 (1969).

[2]H. Feshbach, C. Porter, and V. F. Weisskopf, Phys. Rev. 96, 448 (1954).

[3]H. Feshbach, A. K. Kerman, and R. H. Lemmer, Ann. Phys. (N.Y.) 41, 230 (1967). See also, G. L. Payne, Phys. Rev. 174 (1968) 1227.

[4]Gary T. Mattesich, Lawrence Laboratory Report No. UCRL-75032, 1974 (unpublished).

[5]A. M. Lane and R. G. Thomas, Rev. Mod. Phys. 30, 257 (1958).

[6]H. S. Camarda, Phys. Rev. C 9, 28 (1974).

[7]C. E. Porter and R. G. Thomas, Phys. Rev. 104, 483 (1956).

[8]R. R. Winters, E. D. Earle, J. A. Harvey, and R. Macklin, in Proceedings of the International Conference on the Interaction of Neutrons with Nuclei, 1976, edited by E. Sheldon (unpublished), p. 1260; J. W. Boldeman, A. R. de L. Musgrove, B. J. Allen, J. A. Harvey, and R. L. Macklin, Nucl. Phys. A269, 31 (1976).

[9]H. I. Liou, J. Rainwater, G. Hacken, and U. N. Singh, Phys. Rev. C 12, 102 (1975).

[10]S. Ramavataram, B. Goulard, and J. Bergeron, Nucl. Phys. A207, 140 (1973).

[11]S. Ramavataram, J. Bergeron, M. Divadeenam, and H. W. Newson, Ann. Phys. (N.Y.) 97, 245 (1976).

[12]M. Hasinoff, G. A. Fisher, H. M. Kuan, and S. S. Hanna, Phys. Lett. 30B, 337 (1969).

[13]G. Hacken, H. I. Liou, H. S. Camarda, W. J. Makofski, F. Rahan, J. Rainwater, M. Slagowitz, and S. Wynchank, Phys. Rev. C 10, 1910 (1974).

[14]A. Gilbert and A. G. W. Cameron, Can. J. Phys. 43, 1446 (1965).

[15]J. Gilat, Phys. Rev. C 1, 1432 (1970).